Energy Transfer Studies of the Boundary Layer Interphase in Polystyrene–Poly(methyl methacrylate) Block Copolymer Films

Shaoru Ni, Ping Zhang, Yongcai Wang, and Mitchell A. Winnik*

Department of Chemistry and Erindale College, University of Toronto, 80 St. George Street, Toronto, Ontario, Canada M5S 1A1

Received January 24, 1994; Revised Manuscript Received July 6, 1994®

ABSTRACT: Six pairs of polystyrene–poly(methyl methacrylate) (PS–PMMA) diblock copolymers were prepared with a single fluorescent dye attached to the junction point. One partner contains phenanthrene (the donor), and the other, anthracene (the acceptor). Films were prepared, and nonradiative energy transfer measurements were carried out on these films. Analysis of these data yielded the local concentration of dyes within the interphase. This gives the volume fraction of the interphase in the system, from which we can calculate the ratio R/δ, where δ is the thickness of the interphase and R is the length of the minor phase in the periodic structure of the system. Further analysis of the data in terms of the theory of Ohta and Kawasaki [*Macromolecules* **1986**, *19*, 2621] indicates that R/δ varies as $N^{0.70}$ (predicted, $N^{2/3}$) and δ is about 51 Å. This value is remarkably close to that (50 ± 5 Å) reported by Russell [*J. Chem. Phys.* **1990**, *92*, 5677; *Macromolecules* **1991**, *24*, 5721] from specular neutron reflectivity experiments on similar PS–PMMA diblock copolymers.

Introduction

Block copolymers self-assemble into ordered domains when the product of their chain length N and their chemical interaction potential χ exceeds a critical value ($\chi N > 10.4$).[1] The shapes of these domains are determined exclusively by packing considerations, which in turn depend upon the composition of the block copolymers. For A–B diblock copolymers, regularly spaced spherical domains are formed when the ratio of the block lengths is large. Cylindrical phases form at intermediate block ratios, and when the two arms are nearly equal in length, lamellar phases form. Over a narrow range of compositions between those forming cylinders and lamellae, an ordered bicontinuous double diamond (OBDD) phase has been identified.[2,3]

The past 15 years have seen a rapidly growing interest in block copolymer microphases. The major issues have been associated with determining and predicting morphologies and trying to characterize the interphase separating the two components. One anticipates different behavior in weakly segregated and strongly segregated systems. Beginning with the early theoretical work of Meier[4] and Williams,[5] and the subsequent efforts of Helfand,[6–11] Leibler,[12] and Semenov,[13] the essential features of these systems have been identified. More recent work from Milner et al.,[14,15] Williams,[16] Helfand,[17] Kawasaki,[18–20] Zhulina,[21–23] Olvera de la Cruz,[24,25] Whitmore,[26] Shull,[27] and Noolandi[28] have attempted to provide a more detailed quantitative picture of structure and the locus of the order-to-disorder transition. There have been a number of excellent recent reviews covering various aspects of block copolymer systems.[29]

Transmission electron microscopy and X-ray scattering have played a prominent role as the major experimental techniques used to examine block copolymers in the bulk state. Hashimoto's pioneering experiments are particularly noteworthy.[30–32] More recently, neutron scattering[29] and specular neutron reflectivity[33,34] have been applied with good success to block copolymers in which one component or part of one component was deuterated. Here we consider the possibility that interesting information about these systems might be available through the use of fluorescence spectroscopy to study block copolymers labeled with appropriate fluorescent dyes. We carry out direct nonradiative energy transfer [DET] measurements to examine samples of polystyrene–poly(methyl methacrylate) [PS–PMMA] diblock copolymers containing either a donor dye [D] or an acceptor dye [A] at the PS/PMMA junction. While this system was chosen in part for synthetic convenience, we are fortunate to have the results of Russell and co-workers,[33,34] who have used both neutron scattering and specular neutron reflectivity [SNR] to obtain detailed results about PS–PMMA diblock copolymers with lamellar microstructures.

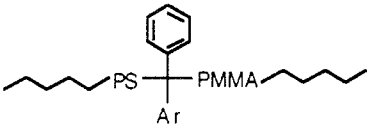

Ar = Phe (1), An (2)

In an energy transfer experiment, one is interested in the time decay of the fluorescence intensity of the donor chromophore [$I_D(t)$] as it is influenced by the presence of nearby acceptors. This decay is governed by the fundamental equation

$$\ln I_D(t) = -\frac{t}{\tau_D} - c_A \int_V \rho(r)(1 - \exp[-w(r)t])\, dr \qquad (1)$$

The $[-t/\tau_D]$ term on the right hand side of eq 1 is simply the unquenched chromophore decay, and our interest is in the second term. Here $\rho(r)$ is the D/A pair distribution, r is the distance separating the centers of the transition moments of a D/A pair, and the term in brackets represents the distance dependence of the energy transfer rate. The term c_A is a dimensionless concentration indicating the mean number of A groups within a distance R_0 (the Förster distance) of each donor.

The rate of energy transfer from D to A by the dipole mechanism has the form

$$w(r) = \frac{3}{2}\frac{\kappa^2}{\tau_D}\left[\frac{R_0}{r}\right]^6 \qquad (2)$$

where τ_D is the lifetime of the donor in the absence of acceptor, and κ^2 is a dimensionless factor describing the interaction strength of two dipoles as a function of their

® Abstract published in *Advance ACS Abstracts*, September 1, 1994.

0024-9297/94/2227-5742$04.50/0

orientation. R_o, the Förster radius, is defined by the expression

$$R_o^6 = \frac{9000 \ln 10 (2/3) \Phi_D}{128 \pi^5 n^4 N_A} \int_0^\infty F_D(\nu) \epsilon_A(\nu) \frac{d\nu}{\nu^4} \quad (3)$$

Here N_A is Avogadro's number, n is the refractive index of the medium, $F_D(\nu)$ is the fluorescence intensity of the donor at the frequency ν normalized to unit area on a wavenumber scale, and ϵ_A is the acceptor molar decadic extinction coefficient. R_o is normally evaluated in the dynamic limit, which assumes that the dipoles reorient much faster than DET takes place. Under these circumstances, one can preaverage the orientation factor to obtain $\langle \kappa^2 \rangle = {}^2/_3$. In the static case, the observable itself has to be averaged over the angular distribution present in the system.

For isotropic energy transfer in Euclidean spaces and in a fractal medium, one obtains, after substitution of these expressions into eq 1 and integration, the Klafter–Blumen equation[37,38]

$$I_D(t) = A_1 \left[\exp\left(-\frac{t}{\tau_D} - P\left(\frac{t}{\tau_D}\right)^\beta \right) \right] \quad (4)$$

In this equation, $\beta = \Delta/6$, with Δ equal to the spatial dimension for DET in one-, two-, or three-dimensional space, and equal to the fractal dimension in a fractal medium. The preexponential term P is a product of an orientation factor

$$g^I = \left(\frac{3}{2} \langle \kappa^2 \rangle \right)^\beta \quad (5)$$

a gamma function $\Gamma(1-\beta)$, and a term c_Δ, a dimensionless concentration, describing the number of acceptors within the critical radius R_o.

$$P = c_\Delta g^I \Gamma(1-\beta) \quad (6)$$

An additional degree of complexity is added if the system is of finite size. Then the distribution $\rho(r)$ explicitly depends upon the position of the excited donor. These systems are encompassed within the term "restricted geometry". Many such systems have been considered from a theoretical point of view. In these instances, one specifies the position of the donor, as, for example, on the surface of a thin cylinder, and carries out the integration over the specific geometry of the system where the acceptors are distributed (e.g. on the surface or within the interior of the cylinder). These analyses also lead to an expression of the form of eq 4, but where the interpretation is more delicate. For example, here Δ becomes an apparent dimensionality whose magnitude may depend upon the locus of a temporal or spatial crossover in the system. If the distribution within the restricted geometry is known, integration over this geometry can be used to obtain independently the parameters to be used in fitting data to eq 4. Alternatively, if the functional form of the distribution $\rho(r)$ is known, the data can be fitted to eq 1 as a means of parameterizing this distribution.

When the detailed shape of the confining space is not known and where one has to consider a distribution of both D and A groups, one has to make further assumptions to proceed. For example, c_Δ is defined as

$$c_\Delta = \frac{\rho_A}{F} \left(\frac{a}{R_o} \right)^\Delta \quad (7)$$

with ρ_A, the number density of acceptors, a, the size of a site (or chromophore) in the system, and F, a shape factor describing the size of a unit sphere in Δ dimensions. The problematic terms in evaluating P are F and g^I. Baumann and Fayer[38] point out that because of the way these terms enter into eq 6, one cannot resolve the separate contributions of F and g^I to P in a time-resolved experiment. These terms must be calculated or inferred from a knowledge of the geometry of the system.

Energy transfer experiments operate in the time domain. Plots of $\log I_D(t)$ vs t are rapidly decaying and featureless. Thus they resemble autocorrelation decay functions in dynamic light scattering experiments. Furthermore, they operate over a limited range of length scales, determined by R_o, the characteristic distance for energy transfer. This aspect offers one significant advantage over scattering experiments in the study of phase-separated systems, especially for nonlamellar systems. DET experiments are blind to the long range order in the system. If a system can be prepared in which the D and A groups are somehow confined to the interphase region, these experiments should allow one to examine these interphases directly. Interpreting scattering experiments in ordered systems requires the assumption that the system has come to equilibrium with respect to its long range order. This is a delicate assumption, especially since polymer diffusion in these systems is slow. One could imagine that the interphase comes to an equilibrium much more rapidly and that information obtained in a DET experiment would be much less sensitive to the need for long term annealing of the samples.

In this report, we describe our initial experiments designed to test the ideas described above. Films were prepared from six pairs of PS–PMMA block copolymers. In each pair, one polymer was labeled with phenanthrene [Phe] as a donor group at the PS/PMMA junction, and the other was labeled with anthracene [An], which acts as the acceptor. Both polymers had similar molecular weights, compositions, and molecular weight distributions. Because of the unique way in which the polymers are labeled, the chromophores report on the location of the joints in the system. If all the junction points are confined to the interphase, the D and A chromophores are likewise confined to the interphase. DET experiments on these films will then provide information about the structure of the interphase in each of the block copolymer samples. This idea is presented pictorially in Figure 1.

There are three approaches one might take in the analysis of fluorescence decay profiles obtained from the block copolymer film samples described above. One might start with eq 1 and try to invert the decay profile to obtain directly the D/A pair distribution $\rho(r)$ within the interphase. This approach is similar to that used in the analysis of dynamic light scattering data where one tries to obtain a distribution of diffusion coefficients from inversion of the autocorrelation signal decay. In both experiments, this is an ill-posed inversion, since the measured decay profile is obtained over a limited range of times. With fluorescence decays, the problem is rendered more difficult because the measured signal is a convolution of the true response of the system convoluted with the instrument response function. Nevertheless, significant progress is being made in the application of distribution analysis to fluorescence decay signals,[35] and we consider this to be one of the long range goals of this research. The most serious problem with this type of analysis is one of establishing that the distribution one obtains from the data is unique and meaningful.

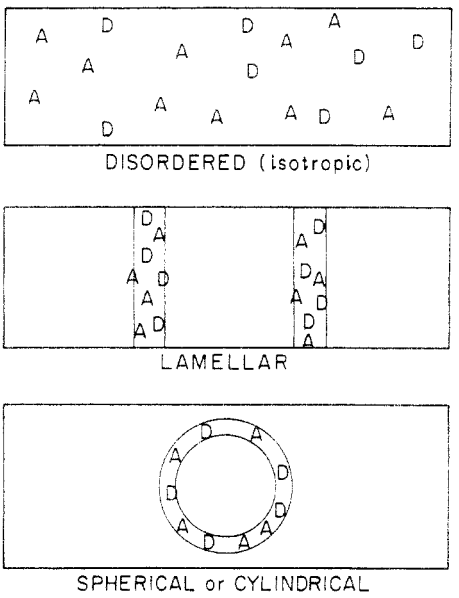

Figure 1. Pictorial representation of the block copolymer morphology with the donor and acceptor dyes confined to the interphase, with local concentrations C_A and C_D and bulk concentrations $C_{A,0}$ and $C_{D,0}$. The ratios $C_D/C_{D,0}$ and $C_A/C_{A,0}$ are equal to the volume fraction of interphase in the system.

With an appropriate theory of the distribution of the joints in the interphase region,[7] one could attempt to derive a functional form for the pair distribution of the joints. This is the distribution $p(r)$ needed to fit data to eq 1. By approaching the problem in this way, one could optimize the parameters describing this distribution and presumably retrieve the parameters which best describe the distribution of the junction points in the interface.

In these initial experiments, we take a more simple approach to the data analysis and examine the system in global terms. In this approach, we employ eq 4 for the analysis of fluorescence decay profiles and extract from the data the molar concentration C_A of acceptor groups in the interphase. The meaningful parameter is the ratio of C_A to $C_{A,0}$, the mean concentration expected if the A groups were not confined to any one phase. This has the effect of treating the system as though there were a quasi-uniform concentration of A groups in the interphase, a kind of step-function model. In the context of this model, the ratio $C_{A,0}/C_A$ is equal to the volume fraction of the interphase in the system. With the help of a geometric analysis for spheres, cylinders, and lamellae, it is then possible to calculate for each sample the ratio R/δ of the interphase thickness to the size of the minor component domain (or to the period spacing) in the system.

Experimental Section

Polymer Synthesis and Characterization. Block copolymers were synthesized by anionic polymerization in tetrahydrofuran [THF] at −78 °C using *sec*-butyllithium as the initiator for styrene polymerization. The procedure follows that previously described:[36] following styrene polymerization, approximately a 2-fold excess of 1-phenyl-1-arylethylene, dissolved in THF, was added to the system. The color change was instantaneous. After an aliquot was removed for analysis, MMA was allowed to distill slowly (from triethylaluminum) into the reaction mixture. The reaction was quenched by addition of an excess of degassed methanol. The polymers were purified by precipitation from THF solution into methanol. Slight traces of PS homopolymer in the samples were removed by extracting the polymer with cyclohexane. The polymers and their characteristics are collected in Table 1.

Table 1. Sample Characteristics for PS–PMMA Diblock Copolymers Labeled at the Junction (An = Anthracene; Phe = Phenanthrene)

sample pair	dye	M_n (PS/PMMA)	M_w/M_n	χN^a	$\Phi_{ps}{}^b$	$f_{ps}{}^b$
C-31	An	3K/29K	1.09	13.3	0.10	0.06
C-32	Phe	3.1K/25K	1.12	11.3		
C-62	An	11K/26K	1.15	14.4	0.32	0.29
C-61	Phe	11K/25K	1.12	14.4		
C-48	An	11K/37K	1.16	20.5	0.25	0.22
C-63	Phe	11K/33K	1.11	17.4		
C-102	An	41K/40K	1.17	30.8	0.54	0.50
C-103	Phe	40K/41K	1.18	30.8		
C-56	An	10K/91K	1.18	39.0	0.12	0.11
C-51	Phe	11K/95K	1.17	41.0		
C-96	An	41K/115K	1.12	59.5	0.29	0.26
C-101	Phe	41K/111K	1.17	57.4		

[a] χ calculated from to $\chi = 0.028 + 3.9/T$ (cf. ref 44). [b] Φ_{ps} and f_{ps} represent the volume and molar fractions of the PS block, respectively.

The polymers were characterized in several ways. An aliquot of the PS block withdrawn from the reaction mixture was analyzed by gel permeation chromatography. This established M_n and M_w/M_n of the PS block. The polymer composition was determined by ^{1}H NMR, and gpc measurements of the block copolymer with tandem UV and refractive index detectors served as a check on M_w/M_n of the block copolymer and the attachment of all fluorescent dyes to the polymer. Model compounds were prepared for the chromophores at the block junction (see below), and their molar extinction coefficients were determined. With these values, we could assess either the degree of chromophore incorporation into the polymer or, assuming complete incorporation, calculate M_n(UV) for the samples.

Synthesis and Characterization of the Model Compounds. The model compounds 1-(2-anthryl)-1-phenylethane and 1-(9-phenanthryl)-1-phenylethane were synthesized by hydrogenation of their unsaturated counterparts[36] 1-(2-anthryl)-1-phenylethylene and 1-(9-phenanthryl)-1-phenylethylene, respectively, in the following procedure: 0.4 g of the starting materials was dissolved in 50 mL of ethyl acetate in a long-neck flask and a small amount of palladium on charcoal (catalyst) was then added. The flask was connected to a conventional hydrogenation apparatus. The flask was filled with hydrogen up to the pressure of a ca. 200 mm column of water and stirred with a magnetic stirrer. The hydrogenation proceeded for 2 h, and then the catalyst was filtered off. White solid products were obtained after the evaporation of the solvent. The raw products were purified by recrystallization from methanol. After recrystallization, the materials were seen to be pure by ^{1}H NMR and showed one spot by thin layer chromatography (TLC). For 1-(2-anthryl)-1-phenylethane: TLC (benzene/hexane 2:5 v/v) one spot, R_f = 0.63; ^{1}H NMR ($CDCl_3$, 400 MHz, TMS) δ (ppm) 8.358 (s, 1H, anthryl H9), 8.340 (s, 1H, anthryl H10), 7.987–7.937, 7.815 (m, 4H, anthryl), 7.436–7.409 (m, 3H, anthryl), 7.295–7.172 (m, 5H, phenyl), 4.324, 4.306, 4.288, 3.878 (q, 1H, methine, J = 7.2 Hz), 1.760, 1.742 (d, 3H, CH_3, J = 7.2 Hz); UV ($CHCl_3$) [λ_{max}, nm (ϵ, L/(mol·cm))] 378 (4050), 358 (5000), 342 (3800), 326 (2200). For 1-(9-phenanthryl)-1-phenylethane: TLC (benzene/hexane 2:5 v/v) one spit, R_f = 0.73; ^{1}H NMR ($CHCl_3$, 400 MHz, TMS): δ (ppm), 8.707, 8.687 (d, 1H, phenanthryl H4, J = 8 Hz), 8.645, 8.627 (d, 1H, phenanthryl H5, J = 8 Hz), 8.142, 8.122, 7.889–7.866, 7.731, 7.624–7.492, 7.316–7.228 (m, 12H, aromatic), 4.929, 4.910, 4.873, 4.854 (q, 1H, methine, J = 7.6 Hz), 1.863, 1.825 (d, 3H, CH_3, J = 7.6 Hz); UV ($CHCl_3$) [λ_{max}, nm (ϵ, L/(mol·cm))] 300 (9400), 298 (8500).

Sample Preparation. Films composed of varying mixtures of matched Phe- and An-labeled block copolymers were prepared by dissolving weighed amounts of each component into toluene to give a final concentration of 1 wt %. A small amount (ca. 0.3 mL) of this solution was placed on a quartz plate (11 × 25 mm) and the solvent was allowed to evaporate slowly over about 4 h. After most of the solvent had evaporated, another aliquot was added, and the process continued until the thickness of the film reached 3–6 μm. The plates were then heated under vacuum at 70 °C for 8 h. Some samples were reannealed for several hours at temperatures well above T_g (e.g. at 130 or 150 °C) before remeasuring their fluorescence decay profiles.

Table 2. Various Quantum Yields and R_0 vs Refractive Indices for Different Polymers

name	n	Φ_f	R_0 (Å)
PMMA	1.4893	0.22	24.5
PS	1.5920	0.25	23.9
(PMMA + PS)/2	1.5406	0.23	24.1

Fluorescence Measurements. Fluorescence spectra were measured with a SPEX Fluorolog 2 instrument equipped with a DMA 3000 data system. Fluorescence decay profiles were measured by the single photon timing technique. Two instruments were employed. Most experiments involved a pulsed lamp (0.5 atm of D_2) as an excitation source. Some experiments were repeated using a picosecond excitation source composed of a mode-locked Nd:YAG laser with a synchronously pumped and cavity dumped dye laser (Rhodamine 6G). In all experiments the excitation wavelength was 298 nm; the emission wavelength was 367 nm (phenanthrene emission), and 20 000 counts were collected in the maximum channel. Data were fitted to models described in the text.

R_0 Determination. UV absorption spectra were measured with a Perkin-Elmer Lambda 19 spectrometer. To determine the donor absorption contribution to the overlap integral, films (ca. 100 μm thick) of the An-labeled polymers (C-102) were prepared by solvent casting. Absorption spectra were measured at several points on the film; and after each spectrum was taken, the film thickness at that point was measured with callipers. Emission spectra were recorded for a similar film prepared from a sample of Phe-labeled polymer (C-103).

Fluorescence quantum yield measurements were carried out on the Phe-labeled block copolymers in solution in toluene, using phenanthrene in cyclohexane (Φ_f = 0.13) as a standard. Two excitation wavelengths were employed: 294.5 nm, which corresponds to a maximum in the phenanthrene absorption and a minimum in the polymer absorption spectrum, and 290 nm, which corresponds to a local minimum in the phenanthrene absorption and a local maximum in the polymer absorption. To minimize errors associated with sharpness of the peaks, narrow slits (1 nm) were used for both sample excitation and emission monochromators. Concentrations were chosen so that the absorbances were less than 0.2, and a standard Beer's law correction was made for the small differences in absorbance at λ_{ex}. In this way we obtain Φ_f = 0.22 for Phe-labeled polymers. To relate the quantum yield of the Phe group in the polymer film to that in solution, we take advantage of the relationship $\Phi_f = k_f\tau_D$, where the radiative rate constant k_f depends only on the refractive index of the medium. Thus the ratio of the Phe lifetimes in solution and in the film can be related to the ratio of the quantum yields, after correcting for the change in local refractive index. Φ_f = 0.23 was obtained, leading to R_0 = 24.1 Å.

The local index of refraction in the interphase is likely to be different from that in either homopolymer phase. Values of Φ_D and of R_0 both depend upon the index of refraction. To indicate the sensitivity of these parameters to the value of n used in the calculations, we collect in Table 2 values obtained by setting n equal to the refractive index of pure PS, pure PMMA, and a 1:1 mixture. In evaluating our data, we assume that the n value corresponding to the 1:1 mixture best describes the interphase environment.

Results and Discussion

Materials and Sample Preparation. The general strategy and experimental details for the synthesis of block copolymers containing D or A groups at the block junction have already been described. In brief, we employ an excess of a 1,1-diphenylethylene analog, 1-aryl-1-phenylethylene (**1**, **2**) to terminate anionic styrene polymerization. This adds one dye-containing unit to the polymer, and the addition product remains sufficiently reactive to initiate methyl methacrylate polymerization. In the case of donor-labeled polymer, the aryl group is 9-phenanthryl. In the case of acceptor-labeled polymer, the aryl group is 2-anthryl.

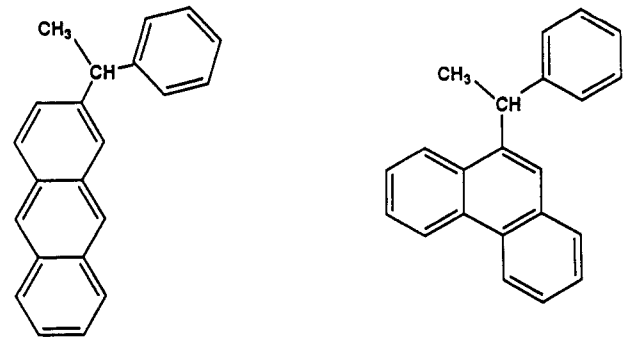

Figure 2. Structures of the two model compounds used for determination of the molar decadic extinction coefficients of the polymer-bound chromophores.

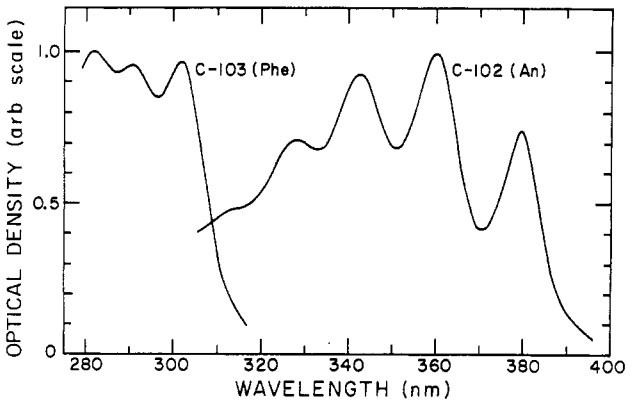

Figure 3. UV absorption spectra of the Phe- and An-labeled polymer samples. Shown here are film samples C-103 (Phe) and C-102 (An). The molar extinction coefficient of C-102 (An) at 359 nm is 6.6×10^3 and it is 10.1×10^3 at 302 nm for C-103 (Phe).

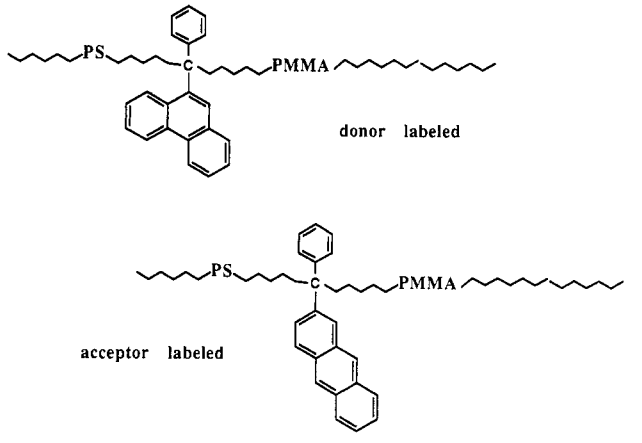

One of the serious challenges was to prepare pairs of block copolymers identical in molecular weight and composition but differing only in the chromophore at the junction. In some instances, we also prepared a third partner, an "unlabeled" polymer, identical to the Phe- and An-labeled materials, but with aryl = phenyl. These polymers and their characteristics are presented in Table 1. To assess the spectroscopy of the system, we also prepared the model compounds **3** and **4**, which contain the essential chromophore unit. These structures are shown in Figure 2.

Absorption and emission spectra for the Phe- and An-labeled polymers are shown in Figures 3 and 4. These spectra are typical of 9-alkylphenanthrene and 2-alkyl-

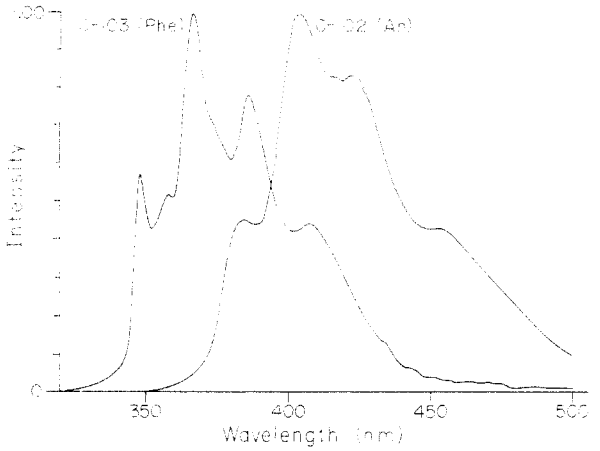

Figure 4. Fluorescence spectra of the two polymers whose absorption spectra are presented in Figure 3.

anthracene derivatives. In previous experiments in our laboratory, an R_0 value of 23 Å was obtained for the model compounds in solution in 1,4-dioxane.[41] The lifetimes of the model phenanthrene compounds in PS or PMMA films (44 ns) are similar to those in solution and to that of the Phe-labeled block copolymer in films, either alone or diluted with unlabeled block copolymer. It should be noted that for PS–(Phe)–PMMA in bulk, the local concentration of Phe groups in the interphase is very much enhanced, which might be expected to lead to some self-quenching of the Phe* emission. Some indication that this effect is present but not very significant is noted in the analysis of the $I_D(t)$ decay curves of the Phe-labeled polymer in bulk. These decays could be fitted to a single exponential form, but the χ^2 values were always higher than those of either the model compounds or the labeled block copolymer in unlabeled matrices.

Films composed of varying mixtures of matched Phe- and An-labeled block copolymers were prepared by solvent casting (toluene, 1 wt %) onto quartz plates. After air drying, the plates were heated under vacuum at 70 °C for 8 h. No differences were observed in the fluorescence signals when the samples were annealed for several hours at temperatures well above T_g (e.g. at 130 or 150 °C). These conditions are significantly milder than those used by Russell to anneal his PS–PMMA samples for SNR measurements.

For PS–PMMA, where Φ_B represents the volume fraction of the minor component, we expect the following types of microstructures:[29]

shape	Φ_B
spheres	<0.17
cylinders	0.18–0.28
OBDD	0.29–0.33
lamellae	0.34–0.50

To assess the validity of these predictions, we have begun a collaboration with the Hashimoto group in Kyoto. At the time of this submission, they have observed the lamellar microstructure of samples C-103 and C-106 by both transmission electron microscopy [TEM] and small angle X-ray scattering.[43] Full details and the results of X-ray scattering experiments will be reported separately.

Microdomain Size/Donor Concentration Relationship. We begin first with a geometric analysis of the relationship between the thickness of the interface δ and the volume fraction of the interphase (V_i/V_o) in the system. We take V_i as the interfacial volume and V_o as the total volume of the system. For lamellar phases, the total area of the lamellae is equal to that of the interphase (Figure 5). If the composition of the block copolymers is unsymmetric, $\Phi_A > \Phi_B$,

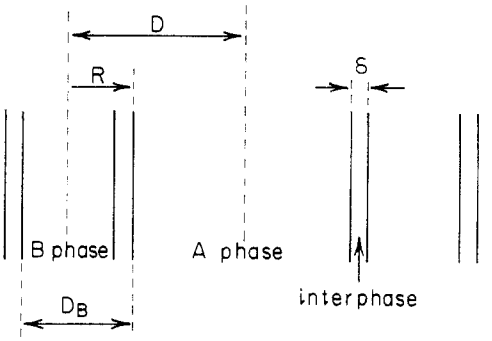

Figure 5. Schematic representation of lamellar geometry.

$$\frac{C_A}{C_{A,0}} = \frac{V_o}{V_i} = \frac{1}{\Phi_B}\frac{R_B}{\delta} = \frac{1}{k\Phi_B} \tag{8}$$

Here R_B is the half-length of the smaller phase, and we define $k = \delta/R_B$.

In the case of cylinders of length L, the interface volume is given by the expression

$$V_i = \pi L[(R+\delta)^2 - R^2] = \pi R^2 L[(1+k)^2 - 1] \tag{9}$$

Defining $k = \delta/R$ and $\lambda = [(1+k)^2 - 1]$, we obtain

$$\frac{C_A}{C_{A,0}} = \frac{V_o}{\pi R^2 L\lambda} = \frac{1}{\lambda\Phi_B} \tag{10}$$

For spherical structures, we have

$$V_i = \frac{4\pi}{3}[(R+\delta)^3 - R^3] = \frac{4\pi R^3}{3}[(1+k)^3 - 1] \tag{11}$$

where k has the same meaning as above. Here we define $\lambda = (1+k)^3 - 1$; thus

$$\frac{C_A}{C_{A,0}} = \frac{V_o}{\frac{4\pi R_o^3}{3}\lambda} = \frac{1}{\lambda\Phi_B} \tag{12}$$

These expressions can be generalized for all the types of microstructures to give

$$\frac{C_A}{C_{A,0}} = \frac{1}{\lambda\Phi_B} \tag{13}$$

with the following definitions for λ:

spheres: $$\lambda = [(1+k)^3 - 1] \tag{14a}$$

cylinders: $$\lambda = [(1+k)^2 - 1] \tag{14b}$$

lamellae: $$\lambda = k \tag{14c}$$

Thus, if we can determine the acceptor concentration in the interphase, C_A, we can obtain the δ/R values through the above relationships. We obtain C_A values through analysis of fluorescence decay curves obtained in the DET experiment.

We have established that P in eq 4 is a parameter associated with the acceptor concentration. The number

of acceptors c_Δ within the critical radius R_0 can be expressed as

$$c_\Delta = \frac{4\pi R_0^3}{3} C_A N_A \tag{15}$$

which, after insertion into eq 6 yields

$$P = P_0 g^I \Gamma(1-\beta) C_A \tag{16}$$

where

$$P_0 = \frac{4\pi R_0^3}{3} N_A$$

By introducing eq 13 into eq 16, we obtain

$$P = \frac{P_0 g^I \Gamma(1-\beta)}{\lambda \Phi_B} C_{A,0} \tag{17}$$

and

$$\lambda = \frac{4\pi R_0^3 \Gamma(1-\beta)\, g^I}{3s\Phi_B} N_A \tag{18}$$

Equation 18 establishes the relationship between the slope s of the P vs $C_{A,0}$ plot and λ; and through λ, the ratio δ/R. Values for δ/R can be obtained from plots of P vs $C_{A,0}$.

Proper data analysis depends upon appropriate values for g^I and R_0. The former is problematic, since the orientation of the chromophores in the interphase is unknown. For a random three-dimensional distribution of orientations,[38] $\langle\kappa^2\rangle = 0.475$, and with $\beta = 0.22$ (see below), $[(3/2)\langle\kappa^2\rangle]^\beta = 0.93$. On the other hand, the chains in the interphase are likely to be stretched. Because of the way in which the chromophores are attached to the backbone, this will promote local conformations in which the chromophores lie flat and parallel to the interface. A random distribution of D/A pairs within a single plane[38] yields $\langle\kappa^2\rangle = 0.946$. In our system this type of orientation would lead to a g^I only slightly bigger than unity. For simplicity in our analysis, we take $g^I = 1.0$. The orientation factor will require more detailed attention in the future.

Data and Data Analysis. Fluorescence decay curves from one set of mixtures obtained in this way is shown in Figure 6. The uppermost line corresponds to a film prepared from the pure Phe-labeled polymer. With no acceptor present, the decay fits well to a single exponential expression with a lifetime τ_D = 44 ns. As An-labeled polymer is incorporated into the system, one observes a more rapid decay component at early times, due to energy transfer in the system. The magnitude of this fast component increases as the An/Phe ratio in the mixture is increased.

The data in Figure 6 and all other $I_D(t)$ profiles for mixtures of Phe- and An-labeled polymers were fitted to eq 4. In all instances reasonable fits were obtained, particularly as judged by the distribution of weighted residuals in the data (cf. Figure 6). More important than the quality of individual fits of the data to a stretched expression is the separation of the variables. One predicts from eq 4 that the β parameter should be a constant, independent of the composition of the mixture, and that P should be proportional to anthracene concentration in the mixture. Excellent agreement with these predictions is obtained. In Figure 7 we show plots of 6β vs $C_{A,0}$ for three block copolymer samples which indicate that the β parameters obtained are constant. Figure 8 demonstrates the linear dependence of P on $C_{A,0}$.

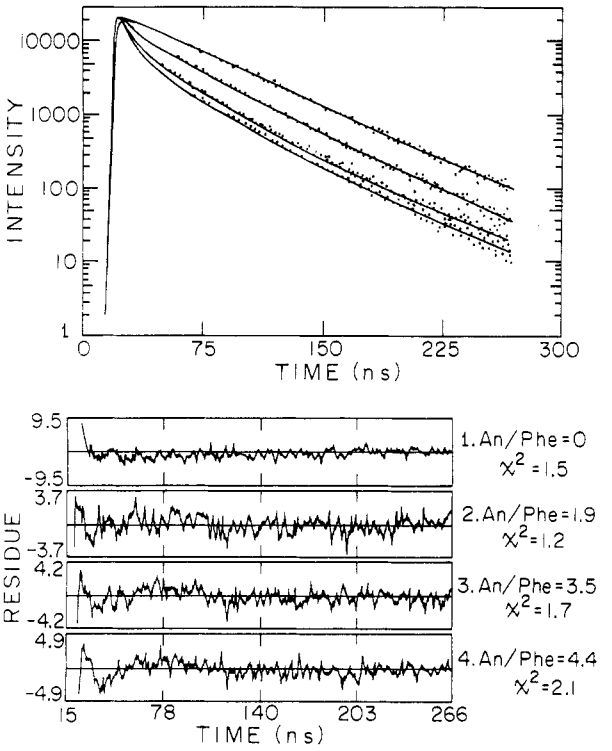

Figure 6. Fluorescence decay profiles of the Phe emission in films composed of various mixtures of Phe- and An-labeled polymers (C-48 and C-63). Top-to-bottom, An/Phe = 0, 1.9, 3.5, 4.4.

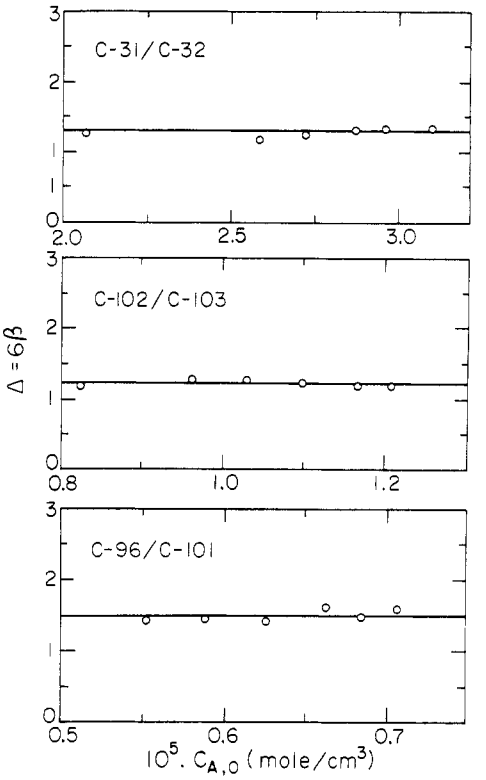

Figure 7. Plot of 6β vs $C_{A,0}$ for three pairs of block copolymer samples.

In every experiment, we find values of β on the order of 0.22. These values are small, and if Δ is thought of as a dimensionality, then the experiment senses a very low dimensionality space. In this type of restricted geometry problem, however, it is not appropriate to consider 6β to

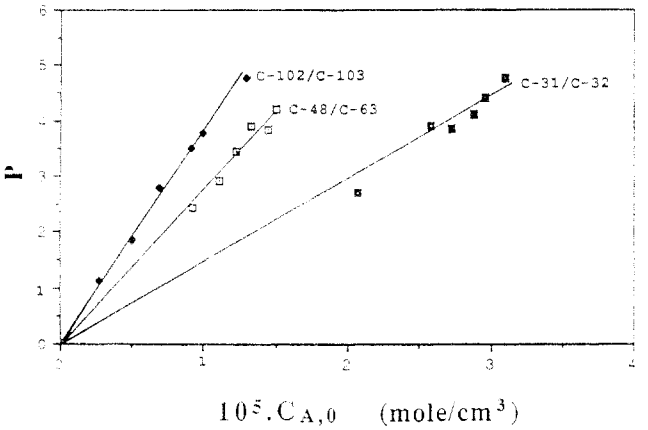

Figure 8. Plot of P vs $C_{A,0}$ for three pairs of block copolymer samples.

be a dimensionality of space. In simulations of DET for D and A groups randomly distributed within spheres,[42] we found similar low values of β for spheres with a radius as large as 5–10 times R_0. To us this indicates that low values of β are due only to edge effects associated with confinement of D and A to a restricted geometry. It also suggests that simulations of DET kinds based upon a theoretical analysis of the shape of the interphase could be a powerful tool for analysis of this type of experiment.

In samples with a high ratio of An/Phe, it becomes meaningful to ask whether there is any evidence for the presence of block copolymer with its junction located outside the interphase. Any donor-labeled polymer with its Phe group outside the interphase will decay with its unquenched lifetime. This will add a weak long tail to the $I_D(t)$ profile. We tested this idea by fitting selected decay profiles to eq 4′ to see if the quality of the fit could be

$$I_D(t) = A_1\left[\exp\left(-\frac{t}{\tau_D} - P\left(\frac{t}{\tau_D}\right)^{\beta}\right)\right] + A_2\exp\left(-\frac{t}{\tau_D}\right) \quad (4')$$

improved. Invariably we found $A_2 \approx 0$, suggesting that not more than ca. 3% of the Phe groups were located outside the interphase.

Theoretical Considerations. In the theoretical analysis of block copolymer morphology by Ohta and Kawasaki [OK],[18] the authors consider a diblock copolymer made up of components of similar Kuhn length b and relate the ratio R/δ to the overall chain length N of the polymer.

$$\frac{R}{\delta} = C\left(\frac{b}{\delta\sqrt{2}}\right)^{4/3}N^{2/3} \quad (19)$$

Expressions similar to eq 19, with R/δ proportional to $N^{2/3}$, are common to all recent theories of block copolymers in the strong segregation limit. This dependence arises from the variation of R with N, since in the theory of strongly segregated systems, δ is found to be, or taken to be, constant. The advantage of the OK contribution for us is that it permits simultaneous analysis of experimental data from block copolymer samples with different morphologies. We can take advantage of this model on two levels. First, our six samples permit us to examine in terms of eq 19 whether R/δ is in fact proportional to $N^{2/3}$. Once this behavior is established, the prefactor in eq 19 allows a value for δ to be calculated. This value can be compared to that reported by Russell[33,34] for PS–PMMA samples giving lamellar microphases.

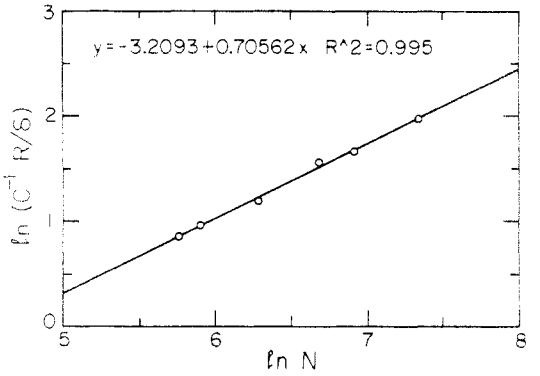

Figure 9. Plot of $\ln(C^{-1}R/\delta)$ vs $\ln N$ for six samples of PS–PMMA. Here R/δ values are calculated using $g^I = 1.0$ and the experimental value $R_0 = 24$ Å.

Equation 19 incorporates a geometry-related constant C dependent upon the mole fraction f and the volume fraction Φ_B of the minor component:

lamellae
$$C = \left[\frac{4\sqrt{2}f(1-f)}{3\Phi_B^2(1-\Phi_B^2)}\right]^{1/3} \quad (20a)$$

cylinders
$$C = \left[\frac{4\sqrt{2}f(1-f)}{9(\Phi_B - \ln\Phi_B - 1)}\right]^{1/3} \quad (20b)$$

spheres
$$C = \left[\frac{4\sqrt{2}f(1-f)}{12\left(\frac{1}{5} - \frac{\Phi_B}{10} - 0.3\Phi_B^{1/3}\right)}\right]^{1/3} \quad (20c)$$

PS–PMMA block copolymers are good examples of block copolymers that satisfy the requirement of the OK theory of similar Kuhn lengths for both blocks. For both polymers one finds a value of $b = 6.7$–6.8 Å, and we use $b = 6.7$ Å.

Periodicity and Interphase Thickness. According to eq 19, one expects a $^2/_3$ power law dependence of (R/δ) on the polymer chain length. Values of λ and (R/δ) for each of our samples are available from the slopes of the plots of P vs $C_{A,0}$. To test the prediction that $R/\delta \sim N^{\alpha}$, with $\alpha = {}^2/_3$, we plot these data according to the expression

$$\ln\frac{1}{C}\frac{R}{\delta} = \text{const} + \alpha\ln N \quad (21)$$

The six points lie on a common line in Figure 9 and the slope is equal to 0.70. Thus the data are in good agreement with the predicted $N^{2/3}$ dependence.

There is ample evidence in support of an $N^{2/3}$ dependence of the period spacing, both from X-ray scattering and from TEM measurements in other systems. The fact that we, too, get a $^2/_3$ power law dependence of R/δ on N (cf. Figure 9) provides strong support for the idea that the interphase is of constant thickness in our samples. The intercept in Figure 9 corresponds to $N = 1$. From the magnitude of the intercept we calculate $\delta = 51$ Å. This value is remarkably close to that (50 ± 5 Å) found by Russell[33,34] from specular neutron reflectivity measurements.

Comments on the Results. Interpretation of P Values. According to eq 6, the P parameter obtained from the fluorescence decay curves is equal to the product of terms which include an orientation parameter g^I, a geometry factor F, and R_0^3. There is a potential uncertainty in each of these terms, and therefore it is necessary to examine how the results depend upon changes in these parameters. Since these terms enter P as a product, it is sufficient to allow one of these parameters to vary. This changes the magnitude of R/δ obtained for each pair of

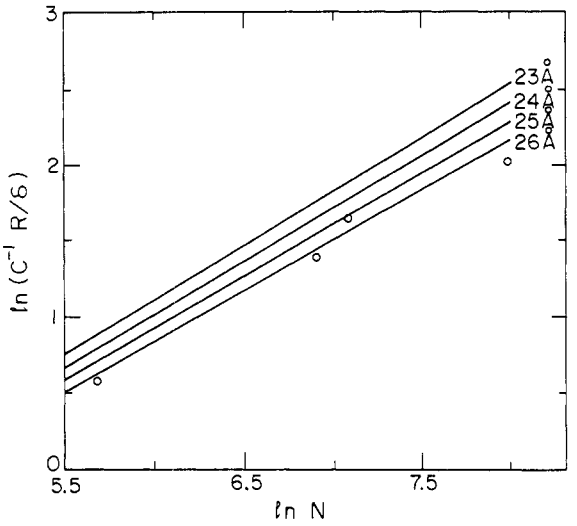

Figure 10. Replot of the $\ln(C^{-1}R/\delta)$ vs $\ln N$ data for PS–PMMA in which R/δ values are recalculated using different values of R_o. Also shown are four data points (O) taken from the neutron reflectivity studies on lamellar PS–PMMA samples by Russell and co-workers.[33,34]

Table 3. Slope (S) of the Plot $\ln(R/\delta C)$ vs $\ln N$ and δ Values Calculated from the Intercepts with Different R_o Values

R_o (Å)	S	δ (Å)
23.0	0.716	51.7
24.0	0.699	51.3
25.0	0.683	51.2
26.0	0.668	51.1
theory	0.667	

block copolymers. In Figure 10, we replot values of $\ln[C^{-1}(R/\delta)]$ vs $\ln N$, with data calculated for various values of R_o. In each instance a straight line is obtained, but the slopes vary slightly with the choice of R_o. The slopes and values of δ calculated from the intercept are collected in Table 3.

Also shown on this plot are data taken from Russell's publications[33,34] for four samples of PS–PMMA which form lamellar phases. These four points fall close to the line obtained from our data with $R_o = 26$ Å. We could generate the same line, keeping $R_o = 24$ Å, by increasing g^I to 1.14. It is interesting that the DET experiments show such concordance with the SNR results. But it is also premature to argue that some adjustment, either in g^I or in R_o, should be made in the interpretation of our results. More significant is the finding that the intercepts, and thus the values of δ, do not depend upon small changes in the components of P. The slopes change because the calculation of R/δ depends upon $P^{1/3}$ for spheres, $P^{1/2}$ for cylinders, and P for lamellae and because of the N values of the particular samples we examine. This suggests that, in the future, a systematic study of PS–PMMA diblocks within a common morphology might provide clarification of this matter.

This entire analysis makes certain simplifying assumptions, the most unrealistic of which is that the acceptor dye can be described by a single concentration parameter in the interphase, implying that it is uniformly distributed. A more sophisiticated analysis of the data should take direct account of the donor–acceptor pair distribution, particularly as it is affected by the detailed shape of the distribution of the junction points in the interphase. We have one experimental check on the validity of this assumption in the context of the current experiments. Inserting the value of $\delta = 50$ Å into eq 19 allows us to calculate a value for R for each of our samples. For sample C-102/C-103, we calculate a spacing of 34.5 nm between the lamellae. SAXS experiments[43] on this sample indicate a lamellar structure and a period spacing of 36.0 nm. These values are in remarkably good agreement considering the difference in the techniques and the various assumptions made here.

Another feature worth noting is the dependence of our results on the theory presented by Ohta and Kawasaki.[18–20] This theory is basically a mean-field approach applicable to weakly segregated systems, to which local interactions to describe the strong segregation limit are simply added. We use this theory not only in fitting our data to eq 19 but also in calculating the C parameters in eq 21. In the OK theory, both polymers are assumed to have equal densities. The differentiation between f and Φ_B is intended to accommodate the presence of A chains in the B-rich phase. We have some evidence suggesting that this presence is negligible; thus we use the densities of the pure components in evaluating C for our six systems.

Strong vs Weak Segregation. Russell and co-workers[34] commented that their lowest molecular weight sample did not satisfy the requirements of the strong segregation limit. They expressed surprise to find that it showed the same interphase thickness and appropriate domain spacing as the higher molecular weight samples. In our lowest molecular weight sample, we find a volume fraction of the interphase of 40%. For this sample, χN is only slightly larger than 10. Nevertheless, this sample also provides data that fall on the same line in Figures 9 and 10 as the higher molecular weight samples. In calculating $\chi N = 10$, we use χ values[44] obtained with the random phase approximation for neutron scattering from low molecular weight PS–PMMA block copolymers in the homogeneous state. Significantly (2–3-fold) higher values of χ were reported recently based upon PVT and cloud point measurements of PS–PMMA blends.[45] These authors conclude that comparison of absolute χ values "obtained by different methods is nearly impossible because a number of model-dependent quantities are used as segment length or segment volume". Thus, the χN values listed in Table 1 may be underestimated.

Our six samples bridge the transition from the weak to the strong segregation limit. Mean-field theories predict that for strongly asymmetric samples, phase separation requires χN values much larger than 10.4.[26] From this point of view, one might wonder if our two lower molecular weight samples, C-31/C-32 (6 mol % PS) and C-61/C-62 (29 mol % PS) are indeed fully phase separated. There is no doubt, however, that there are strong correlations in these two samples in the position of the junction points. If the polymers in the melt were isotropic in their distribution, analysis of the fluorescence decay curves would yield values of $\beta = 0.5$ and C_A values close to those of $C_{A,0}$. It has been suggested to us that the DET experiment may be picking up fluctuations in the position of the joints which are predicted to occur prior to phase separation.[46] If this were in fact the case, this kind of experiment might be a useful way to study these fluctuations. We are hoping that further information on these systems will become available from SAXS and TEM experiments.

Summary

Fluorescence decay measurements have been carried out on films of PS–PMMA block copolymers. The polymers were labeled at the block junction with a single dye. Each film sample was composed of a mixture of Phe-

and An-labeled polymer and donor and acceptor dyes for DET experiments. The six pairs of samples have block lengths consistent with spherical, cylindrical, and lamellar morphologies. Fluorescence decay profiles were analyzed in terms of a model appropriate for energy transfer in a restricted geometry. From this analysis, the local concentration of the acceptor C_A could be determined. The ratio $C_{A,0}/C_A$ is equal to the volume fraction of interphase in the system. These data could be interpreted in terms of the theory of Ohta and Kawasaki to show that R/δ, the (period spacing)/(interface thickness), increases as $N^{2/3}$ and that $\delta = 50$ Å. These results are very similar to those reported by Russell and co-workers for lamellar PS–PMMA films using specular neutron reflectivity.

Acknowledgment. The authors thank NSERC Canada and the Ontario Centre for Materials research for their support of this research. They also acknowledge very helpful discussions with Professor Hashimoto in Kyoto and with Drs. Noolandi and Shi at Xerox.

References and Notes

(1) Fredrickson, G. H.; Helfand, E. *J. Chem. Phys.* **1987**, *87*, 697.
(2) Hashimoto, T.; Shibayama, F.; Fujimura, M.; Kawai, M. *Mem. Fac. Eng. Kyoto Univ.* **1981**, *43*, 184.
(3) Hasagawa, H.; Tanaka, H.; Yamasaki, K.; Hashimoto, T. *Macromolecules* **1987**, *20*, 1651.
(4) (a) Meier, D. J. *J. Polym. Sci., Part C* **1969**, *26*, 81. (b) Meier, D. J. *Polym. Prepr. (Am. Chem. Soc., Div. Polym. Chem.)* **1970**, *11*, 400.
(5) (a) Leary, D. F.; Williams, M. C. *J. Polym. Sci., Part B* **1970**, *8*, 335. (b) *J. Polym. Sci., Polym. Phys. Ed.* **1973**, *11*, 345.
(6) Helfand, E.; Tagami, Y. *J. Polym. Sci., Part B: Polym. Lett.* **1971**, *9*, 741.
(7) Helfand, E.; Tagami, Y. *J. Chem. Phys.* **1972**, *56*, 3592.
(8) Halfand, E. *Macromolecules* **1975**, *8*, 552.
(9) Helfand, E.; Wasserman, Z. R. *Macromolecules* **1976**, *9*, 879.
(10) Helfand, E.; Wasserman, Z. R. *Macromolecules* **1978**, *11*, 960.
(11) Helfand, E.; Wasserman, Z. R. *Macromolecules* **1980**, *13*, 994.
(12) Leibler, L. *Macromolecules* **1980**, *13*, 1602.
(13) Semenov, A. N. *Sov. Phys., JETP* **1985**, *61*, 733.
(14) (a) Milner, S. T.; Witten, T. A.; Cates, M. E. *Europhys. Lett.* **1988**, *5*, 413. (b) Milner, S. T.; Witten, T. A.; Cates, M. E. *Macromolecules* **1988**, *21*, 2616.
(15) Milner, S. T. *Science* **1991**, *251*, 905.
(16) (a) Spontak, R. J.; Williams, M. C.; Agard, D. A. *Polymer* **1988**, *29*, 387. (b) Henderson, C. P.; Williams, M. C. *Polymer* **1985**, *26*, 2026.
(17) Helfand, E. *Macromolecules* **1992**, *25*, 492.
(18) Ohta, T.; Kawasaki, K. *Macromolecules* **1986**, *19*, 2621.
(19) Kawasaki, K.; Ohta, T.; Kohrogui, M. *Macromolecules* **1988**, *21*, 2972.
(20) Kawasaki, K.; Kawakatsu, T. *Macromolecules* **1990**, *23*, 4006.
(21) Zhulina, E. B.; Borisov, O. V. *J. Colloid Interface Sci.* **1990**, *137*, 495; **1990**, *144*, 507.
(22) Birshtein, T. M.; Liatskaya, Yu. V.; Zhulina, E. B. *Polymer* **1990**, *31*, 2185.
(23) Wijmans, C. M.; Scheutjens, J. M. H. M.; Zhulina, E. B. *Macromolecules* **1992**, *25*, 2657.
(24) Olvera de la Cruz, M. *Phys. Rev. Lett.* **1991**, *67*, 85.
(25) Olvera de la Cruz, M.; Mayers, A. M.; Swift, B. W. *Macromolecules* **1992**, *25*, 944.
(26) (a) Vavasour, J. D.; Whitmore, M. D. *Macromolecules* **1992**, *25*, 5477. (b) Vavasour, J. D.; Whitmore, M. D. *Macromolecules* **1993**, *26*, 7070.
(27) Shull, K. R. *Macromolecules* **1992**, *25*, 2122.
(28) Noolandi, J.; Whitmore, M. D. *Macromolecules* **1990**, *23*, 3321.
(29) Bates, F. S.; Fredrickson, G. H. *Annu. Rev. Phys. Chem.* **1990**, *41*, 525.
(30) Hashimoto, T.; Nagatoshi, K.; Todo, A.; Hasegawa, H.; Kawai, H. *Macromolecules* **1974**, *7*, 364.
(31) Hishimoto, T.; Todo, A.; Itoi, H.; Kawai, H. *Macromolecules* **1977**, *10*, 377.
(32) Hashimoto, T.; Fujimura, M.; Kawai, H. *Macromolecules* **1980**, *13*, 1660.
(33) Anastasiadis, S. H.; Russell, T. P.; Satija, S. K.; Majkrzak, C. F. *J. Chem. Phys.* **1990**, *92*, 5677.
(34) Russell, T. P.; Menelle, A.; Hamilton, W. A.; Smith, G. S.; Satija, S. K.; Majkrzak, C. F. *Macromolecules* **1991**, *24*, 5721.
(35) Siemiarczuk, A.; Ware, W. R.; Liu, Y. S. *J. Phys. Chem.* **1993**, *97*, 8082.
(36) Liu, Y. S.; Li, L.; Ni, S.; Winnik, M. A. *Chem. Phys.* **1993**, *177*, 579.
(37) (a) Ni, S.; Juhué, D.; Moselhy, J.; Wang, Y.; Winnik, M. A. *Macromolecules* **1992**, *25*, 496. (b) Calderara, F.; Hurtrez, G.; Nugay, T.; Riess, G.; Hruska, Z.; Winnik, M. A. *Makromol. Chem.* **1993**, *194*, 1411. (c) Hruska, Z.; Vuillemin, B.; Riess, G.; Kats, A.; Winnik, M. A. *Makromol. Chem.* **1992**, *193*, 1987.
(38) Baumann, J.; Fayer, M. D. *J. Chem. Phys.* **1986**, *85*, 4087.
(39) (a) Klafter, J. M.; Blumen, A. *J. Chem. Phys.* **1984**, *80*, 875. (b) Drake, J.; Klafter, J. M.; Levitz, P. *Science* **1991**, *251*, 1574.
(40) The astute spectroscopist will notice in Figure 5 that the (0,0) band of the anthracene emission is diminished in intensity because of self-absorption. No such effect is seen for the donor emission, which would be a source of artefact: Emission reabsorption has the effect of lengthening the measured decay time. It should be distinguished from self-quenching, which would reduce the measured decay time.
(41) Duhamel, J.; Yekta, A.; Ni, S.; Khayakin, Y.; Winnik, M. A. *Macromolecules* **1993**, *26*, 6255.
(42) Duhamel, J.; Yekta, A.; Winnik, M. A. Submitted for publication.
(43) Hashimoto, T.; Sakamoto, N. Unpublished results.
(44) Russell, T. P.; Hjelm, R. P.; Seeger, P. A. *Macromolecules* **1991**, *24*, 5721.
(45) Kressler, J.; Higashida, N.; Shimomai, K.; Inoue, T.; Ougizawa, T. *Macromolecules* **1994**, *27*, 2448.
(46) Gauger, A.; Weyersberg, A.; Pakula, T. *Makromol. Chem., Theory Simul.* **1993**, *2*, 531.